

Preparation of NiO-YSZ/YSZ bi-layers for solid oxide fuel cells by electrophoretic deposition

Laxmidhar Besra*, Shaowu Zha, Meilin Liu

School of Materials Science and Engineering, Georgia Institute of Technology, 771 Ferst Drive, Atlanta, GA 30332-0245, USA

Received 13 September 2005; received in revised form 22 December 2005; accepted 22 December 2005

Available online 18 April 2006

Abstract

A simple and cost-effective method, starting with electrophoretic deposition (EPD) on a carbon sheet, has been developed for preparation of a NiO-YSZ anode and thin, gas-tight YSZ electrolyte layer on it for use in solid oxide fuel cells (SOFCs). The innovative feature of this approach enables the deposition of anode materials as well as the YSZ electrolyte, which were subsequently co-fired in air at high temperatures to remove the carbon and form an anode-supported dense YSZ electrolyte. A functional SOFC constructed by brush painting a layer of mixed cathode consisting of $\text{La}_{0.8}\text{Sr}_{0.2}\text{MnO}_3$ (LSM) and YSZ on the electrolyte layer followed by firing at 1250°C , displayed a peak power density of 434 mW cm^{-2} at 800°C when tested with H_2 as fuel and ambient air as oxidant.

© 2006 Elsevier B.V. All rights reserved.

Keywords: Electrophoretic deposition; Solid oxide fuel cell; YSZ; NiO; Non-aqueous suspension

1. Introduction

Solid oxide fuel cells (SOFCs) have attracted great attention because of their high energy conversion efficiency, excellent fuel flexibility, and minimal pollutant emission [1–3]. However, the relatively high operating temperature ($800\text{--}1000^\circ\text{C}$) of current SOFCs imposes stringent requirements on materials that significantly increase the cost of SOFC technology [1,4]. Reducing the operating temperature of an SOFC to below 800°C can reduce degradation of cell components, improve flexibility in cell design, and lower the material and manufacturing cost by the use of cheap and readily available materials [5,6]. However, the electrolyte conductivity and electrode kinetics drop significantly with the lowered operating temperatures. This can be overcome by lowering the electrolyte resistance (i.e. ohmic losses across the electrolyte) either by decreasing the electrolyte thickness or by using alternative materials of higher ionic conductivity at lower temperatures. Although it has been proposed elsewhere that LaGaO_3 -based oxides [7] and gadolinium doped

ceria (GDC) [2,8] exhibit high oxide ion conductivity suitable as electrolytes in intermediate temperature SOFCs, the production of thin films of these solid electrolytes at low cost still remains a challenge to the development of commercial SOFCs.

The conventional physical vapor deposition (PVD) methods such as sputtering, pulsed laser deposition, molecular beam epitaxy (MBE) [9,10] and the chemical or electrochemical vapor deposition methods [11–13] including combustion chemical vapor deposition (CCVD) [14], and plasma technologies [15,16] are generally very expensive since they require sophisticated and expensive equipment, making them impracticable for implementation in manufacturing environment. The colloidal deposition routes are simple and less expensive method of processing advanced ceramics [17–19]. Electrophoretic deposition is a colloidal processing method in which the charged particles dispersed in a liquid medium are attracted and deposited onto a conductive and oppositely charged electrode on application of a dc electric field. It has the advantages of short formation time, little restriction in the shape of deposition substrate, suitability for mass production, suitability for deposition of laminates. In addition, there is no requirement of binder burnout because the green coating contains little or no organics. In particular, EPD offers easy control of the thickness and morphology of the deposited films through simple adjustment of the deposition time and applied potential. The principal driving force

* Corresponding author at: Regional Research Laboratory, Council of Scientific and Industrial Research, Bhubaneswar 751013, Orissa, India.
Tel.: +91 674 2581635; fax: +91 674 2581637.

E-mail addresses: ldbbsra@rrlbhu.res.in (L. Besra), sz32@mail.gatech.edu (S. Zha), meilin.liu@mse.gatech.edu (M. Liu).

for electrophoretic deposition is the electric force exerted on charged particles on application of an electric field. The rate of electrophoretic deposition depends primarily on the charges on the particles, the electrophoretic mobility of the particles in the solvent, and the applied electric field. The EPD technique has been used successfully in biomedical applications [20,21], luminescent materials [22–24], gas diffusion electrodes [25], oxidation resistant coatings [26], multi-layer composites [27], oxide nanorods [28], carbon nanotube films [29], functionally graded ceramics [30,31], layered ceramics [32], superconductors [33], piezoelectric materials [34], thick film of silica [35], and nano-size zeolite membranes [36]. Considering these vast fields of application, the EPD technique is being recognized to hold a great potential for economic fabrication of thin, dense electrolyte as well as porous electrodes for SOFC applications. However, in spite of these promises, there seems to be little application of EPD in SOFC technology as evident by the availability of only a handful of related publications [37–49], due possibly to the lack of a viable EPD chemistry and process development for the application. The reported work [37–49] either involved multiple deposition and sintering steps [37–40], use of carbon interlayer sputter deposited by expensive high vacuum sputtering apparatus on the substrate prior to deposition [41–43], long sintering cycles [48], or heat treatments in reducing atmospheres to make the substrates conductive [49] before electrophoretic deposition of electrolyte layer on porous anodes. Zhitomirsky and Petric [46,47] reported the electrophoretic deposition of $\text{La}_{0.85}\text{Sr}_{0.2}\text{Ga}_{0.875}\text{Mg}_{0.125}\text{O}_{3-x}$ (LSGM), $\text{La}_{0.8}\text{Sr}_{0.2}\text{Co}_{0.2}\text{Fe}_{0.8}\text{O}_{3-\delta}$ (LSCF), and $\text{Ce}_{0.8}\text{Gd}_{0.2}\text{O}_{1.9}$ (GDC) on Ni foils and Ni-YSZ substrate, however, the GDC and YSZ films obtained were highly porous even after sintering at 1400°C . Therefore, further optimization of the deposition process and thermal treatment procedures are necessary in order to obtain dense deposits for application as electrolytes in SOFCs.

In this paper we present a simple method, starting with electrophoretic deposition on a carbon sheet, for preparation of porous NiO-YSZ composite anode and also for preparation of thin, dense and gas-tight YSZ electrolyte on it. Conventionally, the electrophoretic deposition method requires an electrically conductive substrate. The innovative feature of the method presented in this paper enables deposition of YSZ on the non-conducting NiO-YSZ composite substrate and eliminates heat treatment at reducing atmosphere before EPD.

2. Experimental

2.1. Materials

The YSZ powder used in this investigation was commercial grade 8 mol% Y_2O_3 stabilized ZrO_2 (Tosoh, TZ-8YS) with average particle size of about $0.5\ \mu\text{m}$. Two types of NiO powders were used. The commercial powder (referred to as NiO-comm hereafter) obtained from J.T. Baker contained relatively larger particles ($<10\ \mu\text{m}$). It was milled in ethanol medium for 96 h to less than $5\ \mu\text{m}$ size. The other batch of NiO powder (referred to as NiO-GNP hereafter) was synthesized in our laboratory using the glycine-nitrate process (GNP) [50]. The detail method and

characteristics of the powder thus prepared has already appeared elsewhere [8]. The powders were first ball-milled in ethanol for 48 h and dried before use. The average particles size of the NiO-GNP was $0.8\ \mu\text{m}$. The organic solvent acetylacetone used as dispersing medium in EPD was obtained from Alfa Aesar, USA.

2.2. Suspension preparation

The first step in electrophoretic deposition is to prepare a stable, agglomerate-free colloidal suspension containing the ceramic particles. The ceramic particles are needed to be dispersed in a suitable solvent which can produce stable suspension as well as enhance deposition rate and produce homogeneous and crack free deposit. For deposition of composite anodes, NiO and YSZ powders were mixed in different ratios (70:30, 60:40 and 50:50 w/w) and dispersed in the solvent by sonicating in a high intensity ultrasonic bath to break up agglomerates. The suspension was equilibrated for 24 h and sonicated again before electrophoretic deposition on the carbon sheet disc. Among several solvents studied, acetylacetone was found to be the best in terms of stability of the suspension and deposition quality. In contrast to many EPD processes where it needs addition of suitable additives like binders, there was no necessity of any dispersing agent or binder addition in this case with acetylacetone as the solvent. It was adequate for development of positive surface charge on YSZ and NiO owing to the presence of some residual water in it which is responsible for charging in a manner similar to that in aqueous medium [51]. The positive charges facilitated migration of the particles towards the oppositely charged cathode during EPD. Therefore, subsequently all the deposition experiments were conducted using acetylacetone as the solvent. The optimal solid concentration suitable for EPD was obtained by trial and error approach and found to be about $10\ \text{g L}^{-1}$. Unless otherwise mentioned, a slurry concentration of $10\ \text{g L}^{-1}$ was used in all the subsequent deposition experiments. YSZ suspension ($10\ \text{g L}^{-1}$) for deposition of YSZ electrolyte on the NiO-YSZ composite substrate, was also prepared similarly in acetylacetone as the solvent.

2.3. Substrate preparation

The substrate for electrophoretic deposition is necessary to be electrically conductive. The substrate for deposition of NiO-YSZ composite anode was made by punching out circular discs from electrode baking carbon sheet (Electrochem Inc., USA) and soaked in the solvent for sufficient time to allow wetting its surface. It was then mounted on the electrode holder for EPD. The green deposit of NiO-YSZ on carbon sheet thus obtained was used as the substrate for the deposition of YSZ electrolyte.

2.4. Deposition procedure

The deposition experiments were conducted using an electrophoretic deposition setup schematically shown in Fig. 1. It consists of two electrode holders made of Teflon, as the principal components. One of the electrodes is fixed and the other

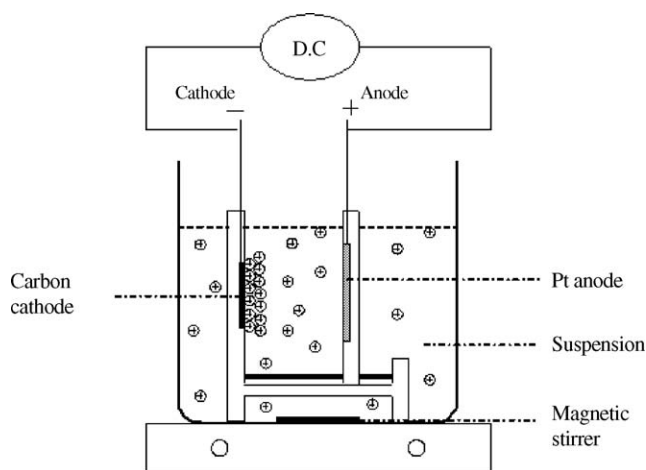


Fig. 1. A schematic diagram of the electrophoretic deposition setup.

is movable and can slide along two parallel rods at the bottom so that the distance between the electrodes can be adjusted to desirable position. Each of the electrode holders has a circular window facing each other to allow fix the electrodes on it. The deposition electrode was mounted on the fixed holder and served as cathode whereas a platinum disc served as the counter-electrode on the movable holder. Unless otherwise mentioned, an electrode spacing of 15 mm was maintained in each of the EPD experiments. The holders along with the electrodes were dipped into the reservoir containing the suspension of YSZ or a mixture of NiO-YSZ. Sedimentation of the particles was prevented by slow stirring by a magnetic bead stirrer as shown in the figure. Electrophoretic deposition experiments were carried out at constant voltages varied in the range from 25 to 500 V, using a high voltage dc power supply unit (Model PS 310) from Stanford Research Systems, USA, with a deposition time from 1 to 3 min. The positively charged NiO and YSZ particles get deposited on the cathode.

2.5. Drying and sintering of deposited film

The green deposits of NiO-YSZ composite and YSZ electrolyte, obtained on carbon discs are first dried in air at room temperature for 24 h, and weighed to obtain the amount deposited. It was followed by heating the sample in air to high temperatures at a rate of $5^{\circ}\text{C min}^{-1}$ and co-sintering at 1400°C for 2 h in a

programmable furnace. The carbon disc gets burnt off during the sintering leaving behind a bi-layer consisting of NiO-YSZ composite layer and a dense layer of YSZ electrolyte on it.

2.6. Microstructural characterization

The microstructures of the deposited films were studied using a Hitachi S-800 scanning electron microscope (SEM). The samples for SEM analysis were gold coated with a sputter coater.

2.7. Fuel cell assembly and testing

A single fuel cell was constructed on the sintered bi-layer by brush painting a cathode layer on the YSZ electrolyte layer followed by sintering at 1250°C . The fuel cell was fixed and sealed to an alumina tube as schematically shown in Fig. 2. A thin layer of silver paste (Heraeus C8710) was used between the NiO-YSZ anode and the ceramic tube in order to prevent gas leakage. The seals were cured as the fuel cell was brought to the testing temperature. Hydrogen gas was used as fuel whereas ambient air served as the oxidant during testing. Air was used as oxidant and was supplied to the cathode by ambient air flow. The cell-tube apparatus was placed in a furnace and brought to the testing temperature with continuous flow of H_2 gas. Platinum wires were attached to each electrode as the output terminal and electrical collector. The fuel cell performance was measured with a Solatron Potentiostat/Galvanostat (Model SI 1287) interfaced with a computer. The impedances were measured typically in the frequency range from 0.1 to 100 kHz using an HF Frequency Response analyzer (Model SI 1255) and the Potentiostat/Galvanostat interfaced with the computer.

3. Results and discussion

3.1. Anode composition

In the anode design of SOFCs, it is important to have the anode conductivity as high as possible. The electrical conductivity of anode is strongly dependent on its microstructure and nickel content. To ensure high conductivity, suspensions with compositions of high NiO:YSZ ratios (70:30, 60:40 and 50:50 w/w) were prepared for EPD experiments. It was found, however, that the properties and composition of NiO used had a significant effect on the quality of deposit and its drying and

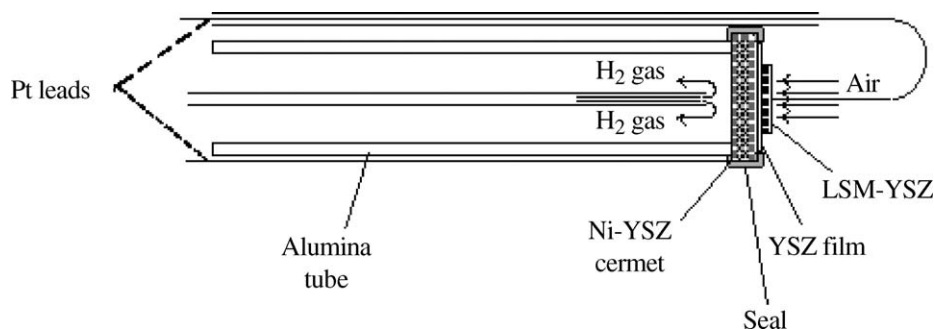


Fig. 2. A schematic diagram showing fuel cell testing assembly.

Table 1
Effect of compositions on drying and sintering characteristics of composite anode

Composition	Drying property
NiO-comm:YSZ (70:30)	Severe cracks
NiO-comm:YSZ (60:40)	Less cracks
NiO-comm:YSZ (50:50)	Very less cracks
NiO-milled:YSZ (70:30)	Less cracks
NiO-milled:YSZ (60:40)	Some micro-cracks
NiO-milled:YSZ (50:50)	Negligible cracks
[NiO-GNP (50%) + NiO-milled (50%)]:YSZ (70:30)	No crack
[NiO-GNP (50%) + NiO-milled (50%)]:YSZ (60:40)	No crack
[NiO-GNP (50%) + NiO-milled (50%)]:YSZ (50:50)	No crack

sintering properties. The use of commercial NiO (NiO-comm) having relatively large particle size ($<10\ \mu\text{m}$) and YSZ in the suspension leads to cracking of the NiO-YSZ deposit which propagated to the electrolyte layer during drying. Higher the NiO content in the suspension, more severe was the cracking (Table 1). As an example, composite deposits obtained from NiO-comm:YSZ (70:30) suspension ($10\ \text{g L}^{-1}$) in acetylacetone, invariably cracked during the room temperature drying, as soon as the solvent gets evaporated. Decreasing the NiO content to 60% in the mixed suspension (i.e. for NiO-comm:YSZ ratio of 60:40), reduced sample cracking considerably but could not eliminate it completely. By further decreasing the NiO content to 50% (i.e. for NiO-comm:YSZ ratio of 50:50), some crack free samples were obtained, but the composition was undesirable for SOFC applications.

One possibility for the anode cracking could be due to non-uniform distribution of NiO particles in the deposit on account of a wide particle size distribution causing non-uniform stress distribution in it. Since we conducted the anode material deposition relatively fast at short deposition time (200 V for 3 min) to obtain a porous anode, it is possible that these non-uniform distributions could occur around coarser NiO particles. At such short deposition times, the fine NiO or YSZ particles could not have occupied best close packing configurations around the coarser NiO particles to prevent formation of these weak spots from which cracks propagate on evaporation of the solvent. However, reduced rates of deposition (through lower applied voltages) performed with the objective of allowing the particles to get deposited at best configuration positions to ensure increased packing density in the deposit, could not prevent cracking considerably.

In a subsequent experiment, the commercial NiO was milled in ethanol medium for 96 h to reduce particle size and its distribution to below $5\ \mu\text{m}$. Once again, anode cracking was reduced considerably, but not eliminated completely (Table 1). Then nano-sized NiO powder obtained from a glycine-nitrate process (NiO-GNP) was used and anode cracking was completely eliminated. Because of the extremely small size of the NiO-GNP powders, however, the anodes were over densified. Finally, we used a mixed powder containing 50 wt.% each of commercial milled NiO and NiO-GNP (arrived at by trials of several compositions). Appropriate amounts of powders were taken from this mixed NiO for use as composite anodes with YSZ for all our subsequent studies.

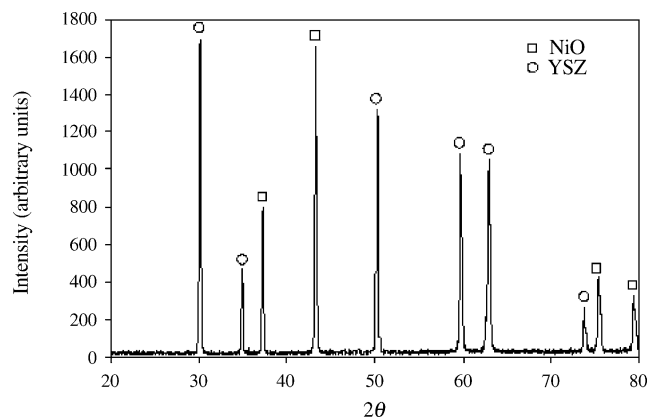


Fig. 3. XRD pattern of composite anode obtained by EPD from 60:40 ratio of NiO and YSZ in acetylacetone, followed by sintering at $1400\ ^\circ\text{C}$ for 2 h.

During electrophoretic deposition although the starting composition of NiO and YSZ in the mixed suspension is known, it is possible that the deposited composition could be very different from the intended composite anode composition depending on the kinetics of deposition of each component, magnitude of zeta potential, and the time of deposition. When the two species in the suspension have a significantly large difference in zeta potential, in spite of them having the same sign of charge, the rate of deposition of the one with higher zeta potential is expected to be higher than the other species. Also, when the time of deposition allowed is different for the two species, the amount deposited would be different. This could result in a deposit with very different NiO:YSZ ratio than anticipated. Therefore, XRD analysis of the mixed deposits was made first to verify that each species was indeed being deposited on carbon substrate. Fig. 3 shows the XRD spectrum for a composite deposit obtained from 60:40 ratio of NiO and YSZ in suspension, followed by sintering at $1400\ ^\circ\text{C}$. It clearly shows all the major characteristic peaks of NiO and YSZ indicating the presence of each species. To determine the mass ratios, we made independent deposition of NiO and YSZ separately from their suspensions ($10\ \text{g L}^{-1}$) in acetylacetone on carbon sheet discs under similar deposition conditions. Fig. 4 shows the weight of NiO and YSZ deposited by such experi-

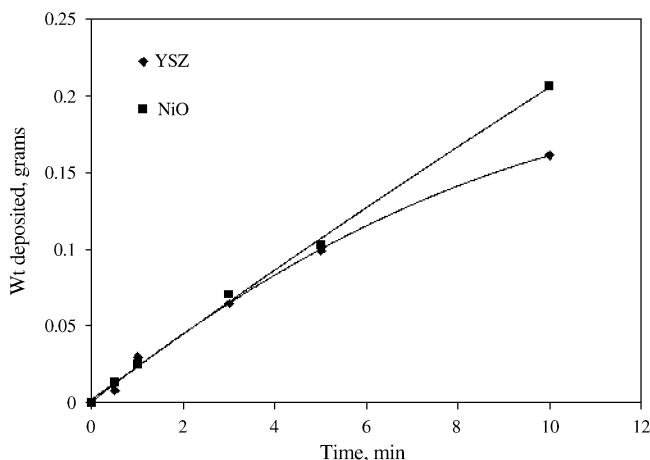


Fig. 4. Rates of NiO and YSZ deposition on carbon paper disc by EPD from their $10\ \text{g L}^{-1}$ suspension in acetylacetone at 200 V.

ment conducted at 200 V for different periods of times. Unlike the reported use of charging agent like iodine [39,40,45] in the electrophoretic deposition of YSZ from acetone or acetylacetone, there was no necessity for addition of any such agent. The positive charge development on both YSZ and NiO surface in acetylacetone were high enough to enable good deposition in a wide range of applied voltages from 25 to 500 V.

It is apparent from the deposition kinetics (Fig. 4) that the deposition of both NiO and YSZ increases linearly with time up to about 5 min, beyond which the rate of YSZ deposition decreases as indicated by a deviation from linearity. This usually happens for constant voltage EPD because of the shielding effect of the deposited layers and accumulation of ions at the electrode [39]. The amount of NiO and YSZ deposited are also very similar and comparable to each other within any deposition time below 5 min. This means that if the deposition behaviors of NiO and YSZ are assumed to be independent of each other, the composition in the deposits are expected to be the same as the composition in the starting suspension. At longer deposition times the rate of YSZ deposition is diminished compared to that of NiO, suggesting that a different composition from that in the suspension is a possibility in the deposit. Assuming non-interference in the deposition behavior of NiO and YSZ from each other in a mixed suspension, the total deposited amount can be estimated as summation of their individual deposition for a given deposition time. Although the assumption may not be strictly realistic considering a fairly high solid concentration (10 g L^{-1}) resulting in electrical double layer interactions, such a computation will serve to provide an idea on the overall deposition behavior from a mixed suspension. Fig. 5 presents the calculated value of percentage NiO in a mixed deposit as a function of NiO/YSZ, obtained from Fig. 4.

Superimposed in Fig. 5 are also the experimentally measured NiO content of mixed deposits obtained by EPD from suspensions containing 70:30, 60:40 and 50:50 ratio of NiO and YSZ in acetylacetone. The NiO content in the mixed deposits were estimated by a simple chemical analysis involving dissolution of a known dried weight of the mixed deposit in a mixture of dilute HNO_3 and H_2SO_4 under mild heating condition wherein

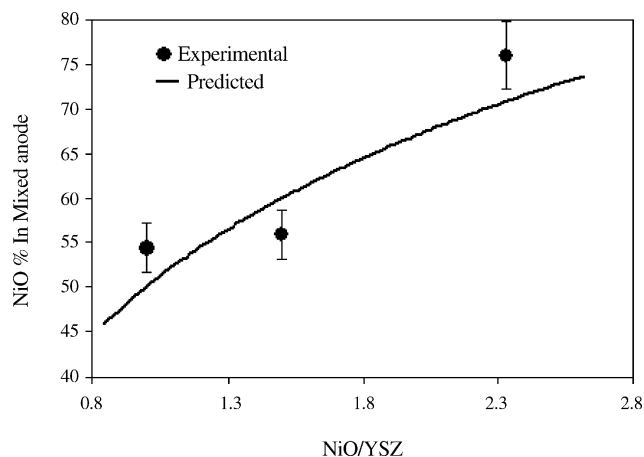


Fig. 5. Variation in NiO content in composite anode as a function of NiO to YSZ ratio.

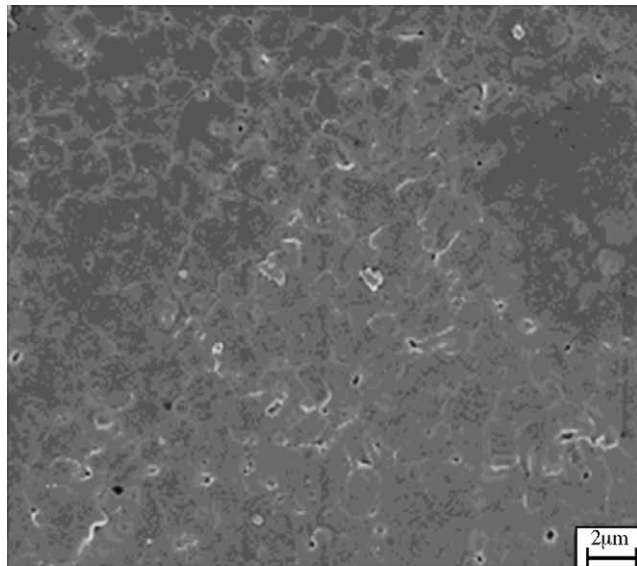
the NiO goes into solution, and can be filtered through a high density filter paper to retain YSZ as residue on it. The filter paper along with the YSZ retained on it is dried and weighed first to estimate the YSZ content. The difference between initial weight and the YSZ content thus obtained is reported as the NiO content in the mixed deposit. It is evident from the figure that the measured NiO content in the composite deposit obtained by EPD are reasonably in agreement with the predicted values.

3.2. Electrolyte deposition

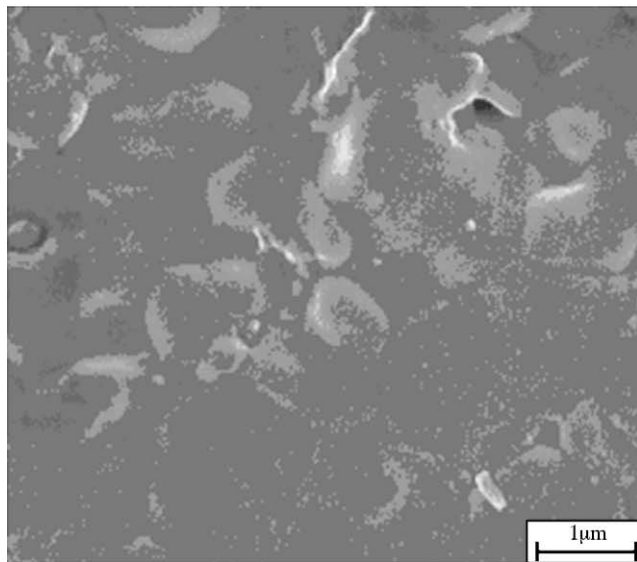
Following the preparation of NiO-YSZ composite, the depositions of thin films of YSZ on them were also made by electrophoretic deposition. This was done by transferring the cleaned electrode holders along with the composite deposit, into the reservoir containing YSZ suspension (10 g L^{-1} in acetylacetone), followed by conducting EPD under desirable conditions. The deposition of YSZ on the composite substrate depended on the drying state of the substrate. It was almost impossible to deposit any YSZ on the composite substrate when it is completely dried before dipping into the YSZ suspension. Sometimes the dried NiO-YSZ crumbled and fell apart into pieces as soon as it is lowered into the YSZ suspension. A semi-dried green deposit of the composite NiO-YSZ was found to be ideal substrate for YSZ deposition. It is not only prevented breaking of the anode, but also resulted in a good quality of YSZ deposit. Since the YSZ was deposited on the wet NiO-YSZ substrate, it ensured strong adhesion between the layers during subsequent drying and sintering. The difficulty in deposition on a dried substrate could probably be a result of the non-existence of an active electrical double layer around dried deposited particles which would be touching one another after evaporation of the solvent. Since for EPD, ideally it is necessary that current should be carried by the charged particles [52] and not by the solvent, the absence of an active double layer could prevent transfer of current through them and consequently influence the particle mobility and deposition as well. On the contrary, for a wet substrate the particles are still surrounded by film of liquid around them ensuring availability of an active electrical double layer/charged particles which can facilitate transfer of current through them to the particles in the suspension.

3.3. Microstructure

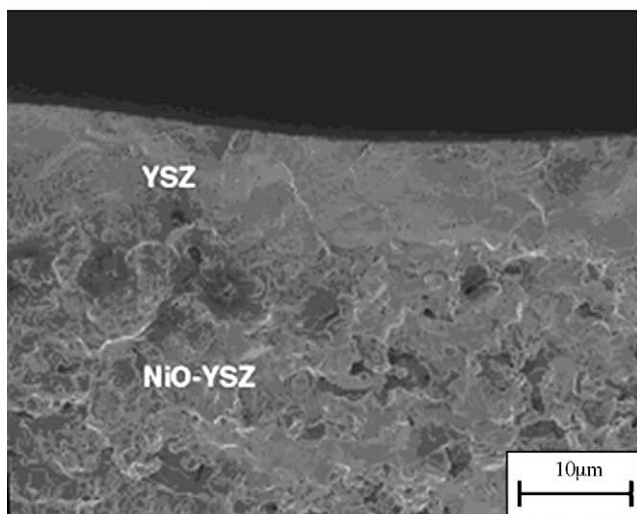
The deposition of YSZ on the composite substrate was found to be in agreement with the observation of previous studies [39,45], and it increased linearly with increasing applied voltage and time up to a certain deposition thickness. The thickness of YSZ film could be easily varied by appropriate increase or decrease in deposition voltage and time. The morphology of the film could also be varied significantly from porous at high voltages to more close packed at low applied voltages. A fully dense YSZ film could be obtained at a single deposition and sintering at 1400°C for 2 h. Films fired below 1400°C for 2 h contained pinholes. Fig. 6 shows the surface and cross sectional morphology of YSZ film on composite NiO-YSZ substrate. No cracks or pores could be observed on the YSZ film. At low mag-



(a)



(b)



(c)

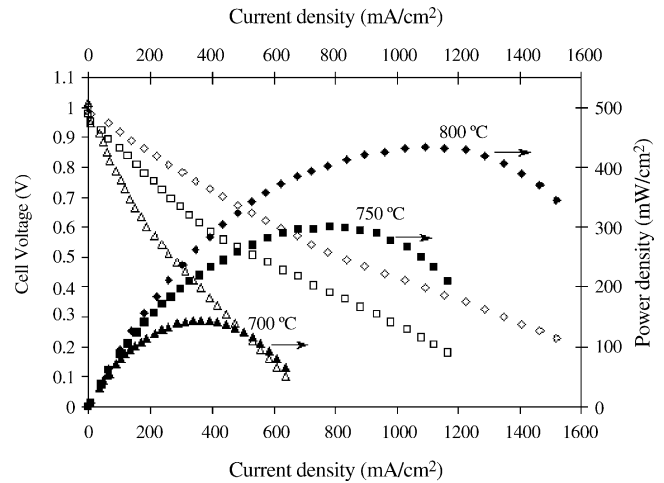


Fig. 7. Cell voltage and power densities as a function of operating current density for a SOFC with configuration of NiO:YSZ (60:40 w/w)/YSZ/LSM-YSZ (50:50 w/w) fuel cells.

nification (Fig. 6a) the surface of YSZ film appears to contain some pinholes in the microstructure. But a close examination of it at higher magnification (Fig. 6b), and from examination of the cross section (Fig. 6c) reveal that they are isolated and are not continuous in nature. This ensures that the YSZ film is sufficiently dense to prevent gas permeation and would serve as a good electrolyte for SOFC. The thickness of the YSZ film was about 10 μm . There is good adherence of the electrolyte to the anode substrate. There are indeed strong interconnections between the YSZ grains of the anode and the electrolyte, which plays a key role in transference of oxygen ions from the electrolyte to the anode during SOFC testing.

3.4. Fuel cell performance

A single fuel cell was constructed on a bi-layer of NiO-YSZ/YSZ co-sintered at 1500 °C for 2 h, by brush painting a composite cathode layer of LSM-YSZ followed by sintering at 1250 °C. The performance of the SOFC, tested in H_2 at varying temperature is shown in Fig. 7. The open circuit voltage of about 1.02 V at 700 °C and 0.99 V at 800 °C suggest that the electrolyte was reasonably dense and gas-tight. The cell showed reasonable power density at 700–800 °C. For example, the peak power density at 700 °C was 144 mW cm^{-2} , and increased to 434 mW cm^{-2} corresponding to a cell voltage of 0.40 V at 800 °C. The performance curves were in concurrence with the impedance spectra shown in Fig. 8, as measured under open circuit condition through 700–800 °C using a two electrode configuration. The intercept with real axis at high frequencies represents the resistance of the electrolyte (R_b) whereas the diameter of the depressed semicircle corresponds to the total impedance of the two interfaces: the cathode–electrolyte inter-

Fig. 6. SEM microphotographs showing morphology of: (a) surface at low magnification, (b) surface at high magnification and (c) cross section of YSZ deposited on NiO-YSZ (60:40) after sintering at 1400 °C for 2 h (EPD condition for NiO-YSZ: 300 V, 3 min; YSZ: 25 V, 2 min).

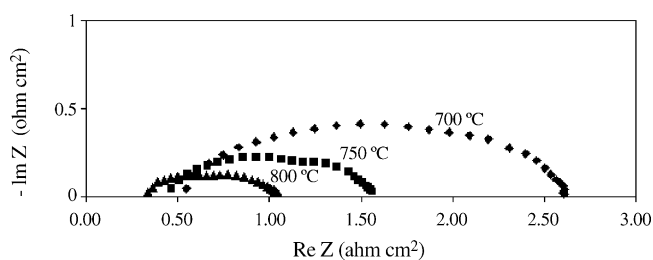


Fig. 8. Typical impedance spectra of a SOFC with configuration of NiO:YSZ (60:40 w/w)/YSZ/LSM-YSZ (50:50 w/w) under open circuit condition using a two electrode configuration.

face (R_c) and the anode–electrolyte interface (R_a). Decreasing the total interfacial impedance of an SOFC is one of the major challenges facing the development of low-temperature SOFCs. A significant decrease in the interfacial impedance could lead to a substantial increase in the cell performance. Table 2 gives the total interfacial resistance of the cell after testing under H_2 atmosphere at different temperatures. The interfacial resistance values are slightly lower than the values reported in literature for same temperatures for cells fabricated by dry pressing [53].

The ionic conductivity of the gas-tight YSZ electrolyte was determined from the impedance data obtained at different temperatures. Knowing the thickness (L) and area (A) in contact with the cathode, we computed the conductivity (σ) according to: $[\sigma = (1/R)(L/A)]$. The conductivity of YSZ as a function of temperature typically follows Arrhenius-type behavior [3]:

$$\sigma T = A_0 \exp\left(\frac{-E_a}{kT}\right)$$

where k is the Boltzmann constant, A_0 the pre-exponential constant, and E_a is the activation energy for conduction. Shown in Fig. 9 is an Arrhenius plot of the conductivities of YSZ made by EPD in the temperature range studied. Superimposed in Fig. 9 are also the conductivities reported in the literature [54] for YSZ membrane deposited on NiO-YSZ pellet by dip coating and co-fired at 1400 °C for 5 h, and those of bulk YSZ pellets made from dried powder and sintered at 1100 °C for 3 h. For the whole range of temperature studied, the YSZ electrolyte produced by EPD has lower conductivity than the bulk YSZ, but has a higher conductivity than the YSZ membrane produced by dip coating. Activation energy (E_a) for conductivity was calculated from the slope of the Arrhenius plots in Fig. 9. It shows that the YSZ electrolyte made by EPD has almost similar activation energy of 85.6 kJ mol⁻¹ compared to values of 87.5 and 88.1 kJ mol⁻¹ reported for bulk YSZ pellet and YSZ membrane, respectively.

Table 2

Total interfacial resistance of the cell

Temperature (°C)	Interfacial resistance ($\Omega \text{ cm}^2$)	
	This work	Reference [53]
800	0.72	0.82
750	1.12	1.48
700	2.08	3.20

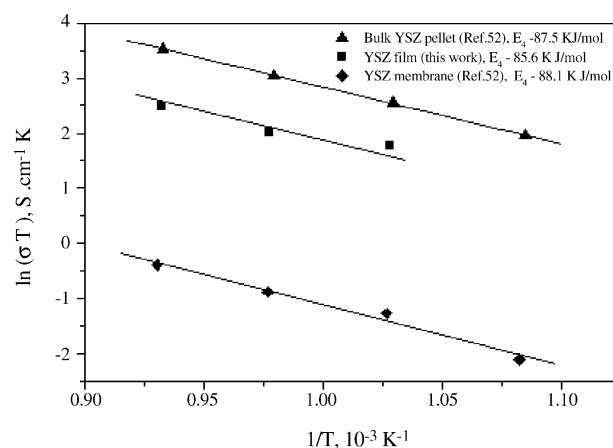


Fig. 9. Arrhenius plots for conductivities of YSZ electrolytes fabricated using different methods: dry pressing [54], colloidal coating [54] and EPD.

The microstructure of electrodes and electrolyte plays a vital role in determining the performance of an SOFC. It is desirable that the anode be porous to allow diffusion of fuel gas through it to facilitate maximum electro-catalytic reactions at the composite anode as well as at the anode electrolyte interface. Fig. 10 shows all the three layers of cathode, electrolyte and anode of the fuel cell after testing under H_2 atmosphere. Both cathode–electrolyte as well as the anode–electrolyte interface show good interfacial adhesion. While the electrolyte is relatively dense and gas-tight, the microstructure of the anode appears less porous than desirable. The nano-sized NiO particles in NiO-YSZ easily tend to grow into larger grain size during sintering process, because densification temperature of NiO is apparently lower than that of YSZ. Such densified anode microstructures increase the resistance to fuel gas diffusion, leading to a moderate performance of the fuel cell. While the performance is to be further improved by tailoring the composition and microstructure of the electrode/interfaces, it is demonstrated

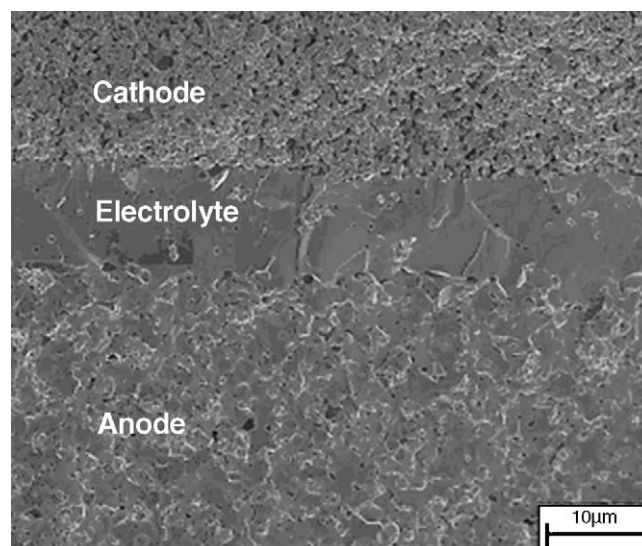


Fig. 10. A cross sectional view (SEM) of Ni-YSZ/YSZ/LSM-YSZ after testing under H_2 atmosphere at 800 °C for 2 h.

that EPD is a viable technique for cost-effective fabrication of SOFCs.

4. Conclusions

Dense/gas-tight YSZ films of about 10 μm have been deposited on a NiO-YSZ composite anode by electrophoretic deposition from a YSZ suspension in acetylacetone, followed by sintering at temperatures higher than 1400 °C. Since the NiO-YSZ anode was also made by the EPD process, and the YSZ was deposited before drying of the composite substrate, a good anode electrolyte bonding could be achieved on subsequent drying and sintering. A single SOFC based on such a bi-layer produced a peak power density of about 434 mW cm^{-2} at 800 °C with H_2 gas as the fuel and stationary air as the oxidant. The SOFC performance could be possibly improved further through tailoring anode composition and microstructure.

Acknowledgements

The authors are thankful to Mr. Ying Liu for assistance in obtaining SEM pictures. One of the authors (LB) is thankful to the Department of Science and Technology (DST), Government of India, for the BOYSCAST fellowship. This work was supported by the US Department of Energy SECA Core Technology Program (under Award no. DE-FC26-02NT41572).

References

- [1] A.B. Stambouli, E. Traversa, *Renew. Sust. Energy Rev.* 6 (2002) 433–455.
- [2] B.C.H. Steele, A. Heinzel, *Nature* 414 (2001) 345–352.
- [3] N.Q. Minh, T. Takahashi, *Science and Technology of Ceramic Fuel Cells*, Elsevier, Amsterdam, The Netherlands, 1995.
- [4] M. Dokiya, *Solid State Ionics* 152 (2002) 383–392.
- [5] B.C.H. Steele, in: U. Bossel (Ed.), *Proceedings of the First European Solid Oxide Fuel Cell Forum*, European SOFC Forum, Oberrohrdorf, Switzerland, 1994, p. 375.
- [6] H.P. Buckkremer, U. Diekmann, L.G.J. DeHaart, H. Kabs, U. Stimming, D. Stoeber, in: V. Stimming, S.C. Singhal, H. Tagawa, W. Lehnert (Eds.), *Proceedings of the Fifth International Symposium Solid Oxide Fuel Cells (SOFC-V)*, The Electrochemical Society, Pennington, NJ, 1997, p. 160.
- [7] T. Ishihara, M. Honda, T. Shibayama, H. Minami, H. Nishiguchi, Y. Takita, *J. Electrochem. Soc.* 145 (1998) 3177–3183.
- [8] S. Zha, W. Rauch, M. Liu, *Solid State Ionics* 166 (2004) 241–250.
- [9] J. Will, A. Mitterdorfer, C. Kleinlogel, D. Perednis, L.J. Gauckler, *Solid State Ionics* 131 (2000) 79–96.
- [10] X. Chen, N. Wu, A. Ignatiev, US Patent 6,645,656 B1 (November 11, 2003).
- [11] U.B. Pal, S.C. Singhal, *J. Electrochem. Soc.* 137 (1990) 2937–2941.
- [12] M. Inaba, A. Mineshige, T. Maeda, *Solid State Ionics* 104 (1997) 303–310.
- [13] M. Aizawa, C. Kobayashi, H. Yamane, T. Hirai, *J. Ceram. Soc., Jpn.* 101 (1993) 237–239.
- [14] Z. Xu, J. Shankar, S. Yarmolenko, *Surf. Coat. Technol.* 177 (2004) 52–59.
- [15] Z. Ogumi, Y. Uchimoto, Y. Tsuji, Z. Takehara, *J. Appl. Phys.* 72 (1992) 1577–1582.
- [16] H. Tsukuda, A. Notomi, N. Hisatome, *J. Therm. Spray Technol.* 9 (2000) 364–368.
- [17] S.N. Heavens, *Electrophoretic deposition as a processing route for ceramics*, in: G.P. Binner (Ed.), *Advanced Ceramic Processing and Technology*, vol. 1, Noyes Publications, Park Ridge, NJ, USA, 1990, pp. 255–283 (Chapter 7).
- [18] S. de Souza, S.J. Visco, L.C. De Jonghe, *Solid State Ionics* 98 (1997) 57–61.
- [19] S. de Souza, S.J. Visco, L.C. De Jonghe, *J. Electrochem. Soc.* 144 (1997) L35–L37.
- [20] M. Wei, A.J. Ruys, B.K. Milthorpe, C.C. Sorrell, J.H. Evans, *J. Sol–Gel Sci. Technol.* 21 (2001) 39–48.
- [21] T.M. Sridhar, U.K. Mudali, *Trans. Indian Inst. Met.* 56 (2003) 221–230.
- [22] J.-H. Yum, S.-Y. Seo, S. Lee, Y.-E. Sung, *J. Electrochem. Soc.* 150 (2003) H47–H52.
- [23] M.J. Shane, J.B. Talbot, B.G. Kinney, E. Sluzky, H.R. Hesse, *J. Colloid Interf. Sci.* 165 (1994) 334–340.
- [24] M.J. Shane, J.B. Talbot, R.G. Schreiber, C.L. Ross, E. Sluzky, K.R. Hesse, *J. Colloid Interf. Sci.* 165 (1994) 325–333.
- [25] K. Hayashi, N. Furuya, *J. Electrochem. Soc.* 151 (2004) A354–A357.
- [26] J.Y. Choudhury, K.N. Rai, H.S. Ray, *Trans. Indian Inst. Met.* 31 (1978) 468–469.
- [27] K. Yamashita, E. Yonehara, X. Ding, M. Nagai, T. Umegaki, M. Matsuda, *Electrophoretic coating of multilayered apatite composite on alumina ceramics*, in: *HA Coating on Alumina Ceramics*, John Wiley and Sons Inc., 1998, pp. 46–53.
- [28] S.J. Limmer, G. Cao, *Adv. Mater.* 15 (2003) 427–431.
- [29] C. Du, D. Heldbrant, N. Pan, *Mater. Lett.* 57 (2002) 434–438.
- [30] S. Put, J. Vleugels, G. Anne, O. Van der Biest, *Colloid Surf. A: Physicochem. Eng. Aspects* 222 (2003) 223–232.
- [31] P. Sarkar, S. Datta, P.S. Nicholson, *Composites, Part B* 28 (1997) 49–56.
- [32] B. Ferrari, A.J. Sanchez-Herencia, R. Moreno, *Mater. Res. Bull.* 33 (1998) 487–499.
- [33] S.K.F. Yau, C.C. Sorrell, *Physica C* 282–287 (1997) 2563–2564.
- [34] J. Van Tassel, C.A. Randall, *J. Eur. Ceram. Soc.* 19 (1999) 955–958.
- [35] K. Hasegawa, S. Kunugi, M. Tatsumisago, T. Minami, *J. Sol–Gel Sci. Technol.* 15 (1999) 243–249.
- [36] W. Shan, Y. Zhang, W. Yang, C. Ke, Z. Gao, Y. Ke, Y. Tang, *Micropor. Mesopor. Mater.* 69 (2004) 35–42.
- [37] T. Ishihara, K. Sato, Y. Mizuhara, Y. Takita, *Chem. Lett.* (1992) 943–946.
- [38] T. Ishihara, K. Shimose, T. Shiomitsu, Y. Takita, in: M. Dokiya, O. Yamamoto, H. Tagawa, S.C. Singhal (Eds.), *Proceedings of the Fourth International Symposium On Solid Oxide Fuel Cells (SOFC-IV)*, 1995, pp. 334–343.
- [39] T. Ishihara, K. Sato, Y. Takita, *J. Am. Ceram. Soc.* 79 (1996) 913–919.
- [40] T. Ishihara, K. Shimose, T. Kudo, H. Nishiguchi, T. Akbay, Y. Takita, *J. Am. Ceram. Soc.* 83 (2000) 1921–1927.
- [41] R.N. Basu, C.A. Randall, M.J. Mayo, *New materials for batteries and fuel cells*, in: *Material Research Society Symposium Proceedings*, vol. 575, San Francisco, USA, 2000, pp. 303–308.
- [42] R.N. Basu, M.J. Mayo, C.A. Randall, US Patent 6,270,642 B1 (August 2001).
- [43] R.N. Basu, C.A. Randall, M.J. Mayo, *J. Am. Ceram. Soc.* 84 (2001) 33–40.
- [44] Z. Peng, M. Liu, *J. Am. Ceram. Soc.* 84 (2001) 283–288.
- [45] F. Chen, M. Liu, *J. Eur. Ceram. Soc.* 21 (2001) 127–134.
- [46] I. Zhitomirsky, A. Petric, *J. Eur. Ceram. Soc.* 20 (2002) 2055–2061.
- [47] I. Zhitomirsky, A. Petric, *J. Mater. Sci.* 39 (2004) 825–831.
- [48] M. Matsuda, O. Ohara, K. Murata, S. Ohara, T. Fukui, M. Miyake, *Electrochem. Solid State Lett.* 6 (7) (2003) A140–A143.
- [49] J. Will, M.K.M. Hruschka, L. Gubler, L.J. Gauckler, *J. Am. Ceram. Soc.* 84 (2002) 328–332.
- [50] C. Xia, M. Liu, *Solid State Ionics* 144 (2001) 249–255.
- [51] L. Vandeperre, C. Zhao, O. Van der Biest, in: Jon Binner (Ed.), *Proceedings of the Novel Chemistry/Processing Session of the Sixth Conference and Exhibition of the European Ceramic Society*, Brighton, UK, June 20–24, 1999, IOM Communications Ltd., London, 2000, pp. 69–74.
- [52] P. Sarkar, P.S. Nicholson, *J. Am. Ceram. Soc.* 79 (8) (1996) 1987–2002.
- [53] Y.J. Leng, S.H. Chan, K.A. Khor, S.P. Jiang, *Int. J. Hydrogen Energy* 29 (2004) 1025–1033.
- [54] C. Xia, S. Zha, W. Yang, R. Peng, D. Peng, G. Meng, *Solid State Ionics* 133 (2000) 287–294.